CRACK ANALYSIS OF MULTICAVITY PRESTRESSED CONCRETE REACTOR VESSELS

R. GALLIX, T.C. LIU and S.C.H. LU
General Atomic Company, San Diego, California 92138, U.S.A.

SUMMARY

A new method to perform the crack analysis of non-axisymmetric, multicavity prestressed concrete reactor vessels (PCRV's) subjected to hypothetical overpressure by using an axisymmetric, two-dimensional finite element computer code is presented. Such analysis is necessary to verify that the PCRV will have a gradual response as its structural capacity is approached and will develop the specified minimum ultimate load capacity.

Concrete, steel liner, bonded reinforcing steel and prestressing steel elements are modeled. The limiting tensile strain criterion is adopted for concrete cracking. The steel elements are assumed to be elastic/perfectly plastic. Von Mises yield criterion and Prandtl-Reuss flow equations define the behavior of the liner in the range of plastic deformations. An orthotropic stress-strain constitutive law is utilized for cracked concrete elements.

To account for the presence of penetrations and secondary cavities in the PCRV, a modified finite element model based on the concept of effective moduli is adopted. The pressure in these cavities is simulated by equivalent axisymmetric pressure distributions. The effect of the non-axisymmetric stress/strain concentrations is simulated by modifying the cracking criterion of appropriate concrete elements, in order to satisfactorily model the onset and propagation of cracks.

In the analysis, the pressure is applied incrementally. For a given pressure, the displacements, strains, and stresses are computed. The state of strains or stresses is then examined against the cracking or yield criteria. If cracking or yield is indicated, the stiffness and load matrices for the cracked and yielding elements are recomputed and a new equilibrium is sought. This procedure is repeated until the desired convergence of the solution is achieved.

The validity of the adopted approach utilizing the two-dimensional finite element method for overpressure analyses of non-axisymmetric PCRV's is demonstrated through comparisons with two multicavity PCRV scale models. A reliable and conservative estimate of PCRV behavior under overpressure is obtained.

1. INTRODUCTION

In the design of a prestressed concrete reactor vessel (PCRV), it is necessary to perform the analysis for the hypothetical overpressure conditions and thus demonstrate structural integrity and a margin of safety at normal working pressure to account for design, construction, operating, and material uncertainties. This paper presents a practical method of obtaining the response of a multicavity PCRV to hypothetical overpressures by using an axisymmetric, two-dimensional non-linear finite element computer code.

The stress-strain relations for the concrete and steel elements, valid throughout the entire range of deformations, are derived. The non-linear finite element formulation for crack analysis of axisymmetric structures is presented. The application of an axisymmetric, finite element computer code to the analysis of multicavity PCRV is discussed in detail. Example analyses and correlations with test data are presented.

2. FINITE ELEMENT ANALYSIS OF AXISYMMETRIC COMPOSITE STRUCTURES

The finite element method has been established in recent years as a powerful analytical tool in generating numerical solutions of linear and non-linear problems in continuum mechanics. This section describes the general finite element formulation for the crack analysis of an axisymmetric composite structure. A composite structure is defined here as a concrete structure consisting of steel liner and reinforcing or prestressing steel members. The method of incremental loading is employed due to the non-linear feature of the problem.

2.1 Finite Element Idealization of Structures

The basic feature of the finite element method is the discretization of the actual structure by a finite number of sub-structures called elements interconnected at certain discrete joints called nodes. The idealized configuration of the structure represents an equivalent mathematical model based on which an approximate numerical solution can be generated for the actual structural problem.

The concrete part of an axisymmetric structure is represented by an assembly of so-called axisymmetric triangular elements. Each element actually is a solid ring with a triangular cross-section. Steel liner is represented by membrane shell elements. The meridional and the circumferential steel members are represented, respectively, by the two-node and the one-node uniaxial bar elements. Two degrees of freedom, the radial and the axial displacements, are considered at each node. The assumed linear displacement field assures constant strains within each element.

2.2 Material Characterization

Concrete is characterized as a non-linear orthotropic elastic material expressed by

$$\underset{\sim}{\sigma} = \underset{\sim}{H}\underset{\sim}{\varepsilon}. \qquad (1)$$

$\underset{\sim}{\sigma}$ is a column matrix composed of the stress components σ_1, σ_2, σ_3, and τ, where σ_1 and σ_3 are two normal stresses and τ is the shear stress in a meridional plane whereas σ_2 is the circumferential stress. $\underset{\sim}{\varepsilon}$ is also a column matrix denoting the equivalent strain components ε_1, ε_2, ε_3, and γ. The material matrix is defined by

$$\underset{\sim}{H} = \begin{bmatrix} e_1C_1 & e_1e_2C_2 & e_1e_3C_2 & o \\ e_2e_1C_2 & e_2C_1 & e_2e_3C_2 & o \\ e_3e_1C_2 & e_3e_2C_2 & e_3C_1 & o \\ o & o & o & e_1e_2C_3 \end{bmatrix} \quad (2)$$

where $$C_1 = \frac{(1-\mu)\ E}{(1+\mu)(1-2\mu)} \quad (3)$$

$$C_2 = \frac{E}{(1+\mu)(1-2\mu)}$$

$$C_3 = \frac{E}{2(1+\mu)}$$

and e_i ($i = 1, 2, 3$) assumes the value of unity or zero indicating respectively the "closing" or "opening" of a crack surface which is perpendicular to ε_i ($i = 1, 2, 3$). The quantities μ and E are the Poisson's ratio and the Young's modulus, respectively. The stress-strain law referring to the global coordinate system adopts the following form

$$\underset{\sim}{\bar{\sigma}} = \underset{\sim}{\bar{H}}\underset{\sim}{\bar{\varepsilon}} \quad (4)$$

where $$\underset{\sim}{\bar{H}} = \underset{\sim}{R}^T\underset{\sim}{H}\underset{\sim}{R} \quad (5)$$

and $\underset{\sim}{R}$ is an orthogonal transformation matrix so defined such that

$$\underset{\sim}{\varepsilon} = \underset{\sim}{k}\underset{\sim}{\bar{\varepsilon}},\ \underset{\sim}{\bar{\sigma}} = \underset{\sim}{R}^T\underset{\sim}{\sigma}. \quad (6)$$

It is easy to show that $\underset{\sim}{\bar{H}} = \underset{\sim}{H}$ if $e_1 = e_2 = e_3 = 1$. In other words, the constitutive equation (1) is isotropic before cracking develops in concrete.

Steel is treated as an elastic and perfectly plastic material. For liner elements the following incremental biaxial stress-strain equation is adopted

$$d\underset{\sim}{\sigma} = \underset{\sim}{H}\ d\underset{\sim}{\varepsilon}. \quad (7)$$

$d\underset{\sim}{\sigma}$ and $d\underset{\sim}{\varepsilon}$ are, respectively, the incremental stress and strain vectors and are defined by

$$d\underset{\sim}{\sigma}^T = \langle\ d\sigma_1 \quad d\sigma_2\ \rangle$$

$$d\underset{\sim}{\varepsilon}^T = \langle\ d\varepsilon_1 \quad d\varepsilon_2\ \rangle \quad (8)$$

where σ_1 and ε_1 are meridional components and σ_2 and ε_2 are circumferential components. $\underset{\sim}{H}$ is the material matrix defined by

$$\underset{\sim}{H} = \underset{\sim}{H}^e + e\ (\underset{\sim}{H}^p - \underset{\sim}{H}^e). \quad (9)$$

$\underset{\sim}{H}^e$ is the usual plane stress elastic material matrix expressed by

$$\underset{\sim}{H}^e = \frac{E}{1-\mu^2} \begin{bmatrix} 1 & \mu \\ \mu & 1 \end{bmatrix}. \quad (10)$$

$\underset{\sim}{H}^p$ on the other hand is the plastic material matrix defined by

$$\underset{\sim}{H}^p = \frac{E}{1-2\ \mu\lambda+\lambda^2} \begin{bmatrix} \lambda^2 & -\lambda \\ -\lambda & 1 \end{bmatrix} \quad (11)$$

where λ is a function of the stress components defined by

$$\lambda = (2\sigma_1-\sigma_2)/(2\sigma_2-\sigma_1). \tag{12}$$

The quantity e which appears in Eq. (9) obtains the value of unity if the material is in the plastic region and if Eq. (7) is applied to a loading process. Otherwise e retains the value of zero and Eq. (7) simply represents a linear elastic biaxial stress-strain equation. For uniaxial bar element, Eq. (7) reduces to

$$d\sigma = (1-e)\ E\ d\varepsilon \tag{13}$$

where σ and ε are the uniaxial stress and strain.

The cracking of a concrete element is determined by comparing the principal tensile strain with the cracking strain obtained from a uniaxial tension test. The yielding of steel elements follows Von Mises criterion which possesses the following yield surface

$$[(\sigma_1-\sigma_2)^2 + \sigma_1\sigma_2]^{1/2} - \sigma_{yd} = 0 \tag{14}$$

where σ_{yd} is the uniaxial yield stress.

2.3 Finite Element Formulation

The equilibrium equations in a finite element structural analysis can be conveniently obtained from the virtual work principle given by

$$\int_V \delta\underset{\sim}{\varepsilon}\ \underset{\sim}{\sigma}\ dv = \delta\underset{\sim}{q}^T\ \underset{\sim}{P} \tag{15}$$

where $\underset{\sim}{\varepsilon}$ indicates the strain components, $\underset{\sim}{\sigma}$ the stress components, $\underset{\sim}{q}$ the nodal displacements, $\underset{\sim}{P}$ the nodal forces, and δ the variational operator. The strain components can be related to the nodal displacements by

$$\underset{\sim}{\varepsilon} = \underset{\sim}{\phi}\ \underset{\sim}{q}. \tag{16}$$

Substituting (16) into (15) leads to the following equilibrium equations

$$\underset{\sim}{P} = \int_V \underset{\sim}{\phi}^T\ \underset{\sim}{\sigma}\ dv \tag{17}$$

or, in terms of incremental quantities

$$d\underset{\sim}{P} = \int_V \underset{\sim}{\phi}^T\ d\underset{\sim}{\sigma}\ dv. \tag{18}$$

Substitution of the stress-strain relations Eq. (1) or Eq. (7) in Eq. (18) yields

$$d\underset{\sim}{P} = \underset{\sim}{K}\ d\underset{\sim}{q} \tag{19}$$

where $\underset{\sim}{K}$, the instantaneous element stiffness matrix is defined by

$$\underset{\sim}{K} = \int_V \underset{\sim}{\phi}^T\ \underset{\sim}{H}\ \underset{\sim}{\phi}\ dv. \tag{20}$$

The force-displacement equation (19) can be obtained for each of the elements. After proper assembly, the global equilibrium equations can be obtained for the entire structural system and the unknown nodal displacements can be solved if the displacement boundary conditions are properly imposed. For known displacements at the nodes, the element strains and stresses can therefore be computed.

2.4 Computer Program SAFE-CRACK

The analytical procedure formerly described can be carried out by the use of the computer program SAFE-CRACK (Ref. 1). A brief summary is presented here to cover the major operation of the program. As noted previously the method of incremental loading is employed because of the non-linear feature of the structural problem. Furthermore, an iterative procedure is conducted within each load increment in order to generate a converged solution. For each cycle of iteration, the following operations are performed:

1. Calculate or update element stiffness matrices and load vectors accounting for cracking and yielding of each element.
2. Assemble element stiffness matrices and load vectors and apply displacement boundary conditions to form the global equilibrium equations.
3. Solve the equilibrium equations to obtain incremental nodal displacements.
4. Compute strains and stresses and check the cracking or yielding situation for each element.

The capability of the computer program SAFE-CRACK in predicting realistic structural response of axisymmetric composite structures subjected to overpressure was demonstrated by applying the analytical method to the single-cavity PCRV test model described in Ref. 6. Close agreement between the analytical and experimental results was obtained (Ref. 1).

3. ANALYTICAL REPRESENTATION OF MULTICAVITY PCRV

A multicavity PCRV, by nature of its geometrical configuration, cannot be treated as an axisymmetric structure (Fig. 1). Three dimensional analysis is required to predict correctly the state of stress in this type of structure. A comprehensive three-dimensional non-linear finite element analysis involves very elaborate and time-consuming computerized procedures. Consequently, a series of modifications has been devised for the application of an axisymmetric, two-dimensional finite element analysis to multicavity PCRVs.

3.1 Refueling Penetrations and Secondary Cavities

In order to simulate the effect of the presence of the refueling penetrations, steam generator and auxiliary cooling loop cavities and their cross-ducts on the overall stiffness of the vessel, equivalent Young's moduli are used in the corresponding regions of the finite element model (Fig. 2a).

In the top head the perforated refueling penetration zone is replaced with a solid zone of constant equivalent modulus (E*) which accounts for the steel penetration liners and provide the same overall radial, circumferential and bending stiffnesses. This modulus is calculated according to Ref. 2, 3 or 4 which yield nearly the same values.

For the steam generator and auxiliary cavities and their cross-ducts a parametric study showed that reducing the elastic modulus of each concrete element in these regions by the ratio of the solid to the total circumference around the PCRV at the center of gravity of the element yields results in good agreement with experimental data, both in the elastic and in the cracked states. It was also found that the value of the equivalent modulus E** has a relatively minor influence on the behavior of the model.

3.2 Stress Concentrations in the Non-axisymmetric Regions

Concentration of circumferential tensile stresses which cause cracking in the concrete ligaments adjacent to the secondary cavities of multicavity PCRV's subjected to overpressurization have been illustrated by planar and three-dimensional analyses as well as by model tests. However, in axisymmetric analytical models the hoop stresses are constant around the vessel. This absence of stress concentration is compensated by lowering the cracking criterion so that cracks will appear and develop in the finite element model at the same pressures as they do in the actual vessel. Fig. 2b shows the regions where the uniaxial tensile strain of concrete has been assumed equal to zero.

3.3 Pressure on the Walls of the Refueling Penetrations and the Secondary Cavities

Equivalent axisymmetric pressure distributions are used to produce the same overall effect on the model as the actual pressure distributions have on the vessel (Fig. 3a).

The outward thrust exerted by the pressurized refueling penetration region on the peripheral zone of the top head is determined by using the formula for the uniform radial stress in the equivalent solid plate given in Ref. 2.

The vertical upward and downward resultants of the pressure on the walls of the cross-ducts are replaced with equivalent pressure distribution on horizontal ring surfaces at the top and bottom generatrices of the ducts.

The vertical pressure forces on the secondary cavity closures are assumed distributed over similar axisymmetric surfaces at the level of the shear anchors.

As for the pressure acting on the walls of the secondary cavities, a special study was conducted to determine the equivalent axisymmetric pressure distribution. There are two aspects to this problem: firstly the pressure tends to split the wall of the vessel along a vertical cylindrical surface through the centerline of the cavities; secondly it produces an overall outward deflection of the whole wall. The first effect is simulated by applying to the model two equivalent "splitting" axisymmetric pressure distributions p_1 and p_2 whose resultant on any sector of the vessel is null, as shown on Fig. 3b. Another, outward directed axisymmetric pressure distribution, p_3, is added, as shown on the same figure, to obtain the correct radial deflections. The intensity of p_3 is determined by a comparative, parametric study of a horizontal section of the barrel wall. A planar finite element model representing the actual wall configuration and pressure loading and an axisymmetric model representing the corresponding section of the finite element model used for the crack analysis of the vessel's top half are analyzed (Fig. 4 a, b). The deflections obtained in both cases are shown on Fig. 4.c for various values of p_3. It can be seen that for the vessel configuration in question the value p_3 = 0.3465 x (actual pressure) gives the best results.

4. EXAMPLE ANALYSES

4.1 Hartlepool 1/10th Scale PCRV Model

A 1/10th scale PCRV model of Hartlepool 625 MW(e) AGR system, Fig. 5, was constructed and tested by Taylor Woodrow Construction Ltd. (TWC), England, in 1968 (Ref. 5). The finite element model for the crack analysis using the SAFE-CRACK computer program is shown in Fig. 6. Invoking the conditions of symmetry, only the upper half of the vessel is considered. Liner and deformed reinforcement are modeled. The reinforcing effect of the refueling penetrations and the cross-ducts in their longitudinal direction is also modeled with bar elements. Prestress is applied by imposing adequate negative thermal strains to the prestressing bar elements. Some typical results are compared with the test data (Fig. 7 and 8). The method gives a good approximation of the model's behavior under overpressure.

4.2 1/20th Scale HTGR Model PCRV

Ohbayashi-Gumi Ltd. of Japan, built and tested in 1973 a 1/10th scale model of the 1160 MW(e) HTGR PCRV (Fig. 9). A crack analysis of this model was performed, using the same approach as for Hartlepool model.

Results are compared with the experimental data reported in Ref. 6 on Fig. 10. Figure 11 illustrates the crack patterns. Again the method yields an accurate and conservative solution.

5. CONCLUSION

The two-dimensional computer code SAFE-CRACK was used to analyze the behavior of multicavity PCRVs subjected to overpressurization. A practical method of replacing the non-axisymmetric features of the vessels with equivalent, axisymmetric ones was developed. This method was validated by comparison with data obtained from tests of representative scale models. It allows a simplified analysis of the PCRVs, taking into consideration cracking of concrete and yielding of prestress, liner and deformed reinforcement. Therefore it constitutes a practical tool to investigate the behavior of the vessels beyond the elastic domain and to verify whether a given design satisfies the prescribed safety criteria.

REFERENCES

[1] LU, S. C. and CHARMAN, C. M., "SAFE-CRACK Users' Manual," General Atomic Company, Report No. GA-A13035, December 1974.

[2] ASME Boiler and Pressure Vessel Code, Section III, Art. A-8000, 1971.

[3] BAILEY, R. W. and FIDLER, R., "Stress Analysis of Plates and Shells Containing Patterns of Reinforced Holes," Nuclear Engineering and Design, Vol. 3, 1966 (pp. 41-53).

[4] HARROP, J., "Analysis of the Standpipe Zone of Prestressed Concrete Vessels," Journal of the Prestressed Concrete Institute, June 1969 (pp. 64-73).

[5] LANGAN, D. and SMITH, J. R., "1/10th Scale Model of Hartlepool Pressure Vessel - Introduction Statement," Structure Research Laboratory, Taylor Woodrow Construction Ltd., 6th November 1968.

[6] TAKEDA, T. et al, "Pressure Tests of PCRV Models," Paper presented at the 7th FIP International Conference, New York, May 1974.

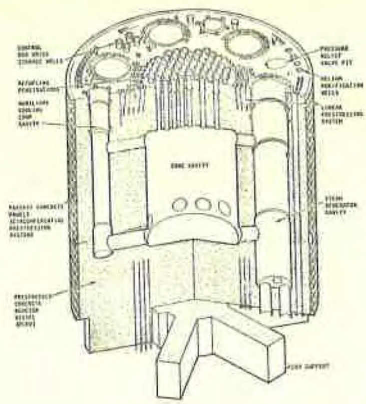

Fig 1 General PCRV Arrangement

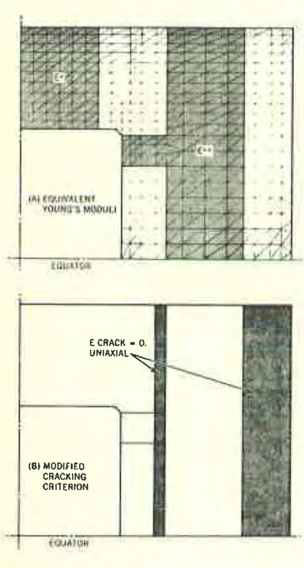

Fig 2 Equivalent Young's Moduli and Concrete Cracking Criterion

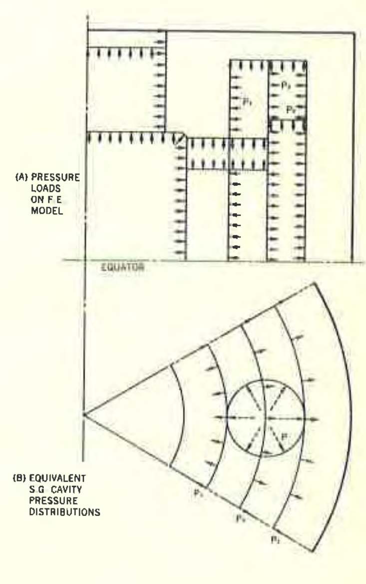

Fig 3 Equivalent Pressure Loads

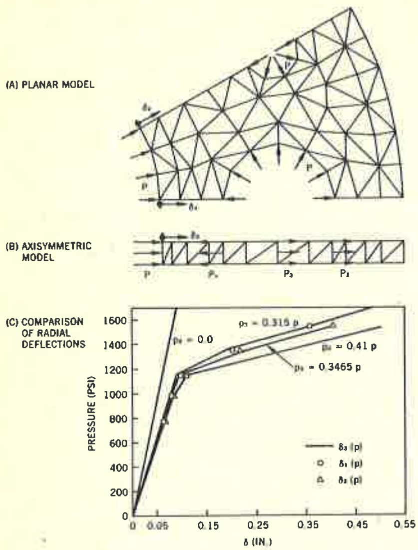

Fig 4 Equivalent Axisymmetric Pressure Distribution

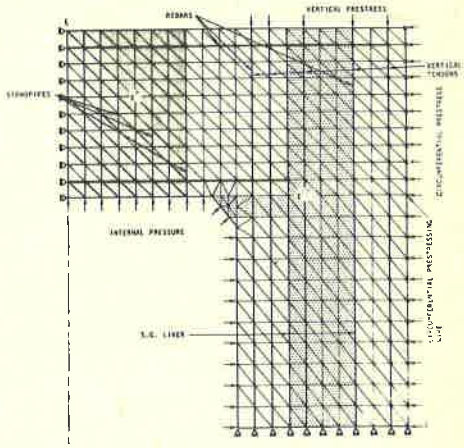

Fig 6 Finite Element Idealization of Hartlepool PCRV Model

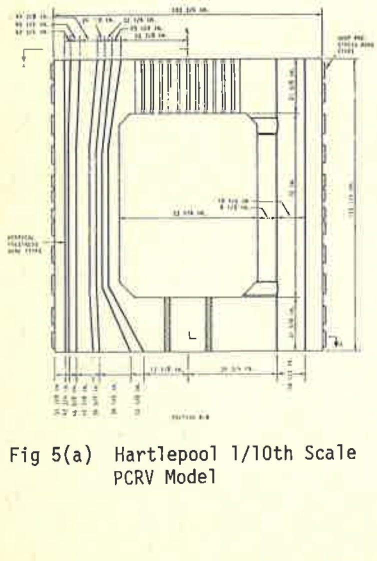

Fig 5(a) Hartlepool 1/10th Scale PCRV Model

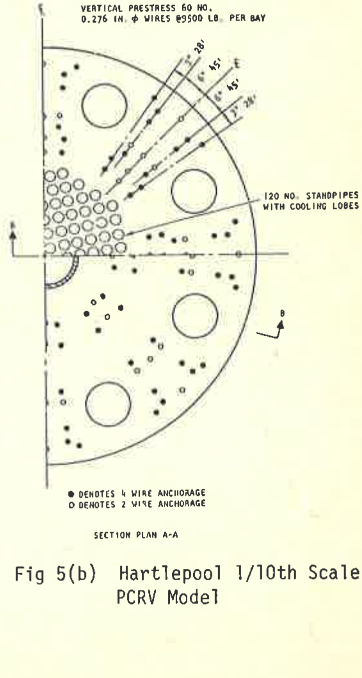

Fig 5(b) Hartlepool 1/10th Scale PCRV Model

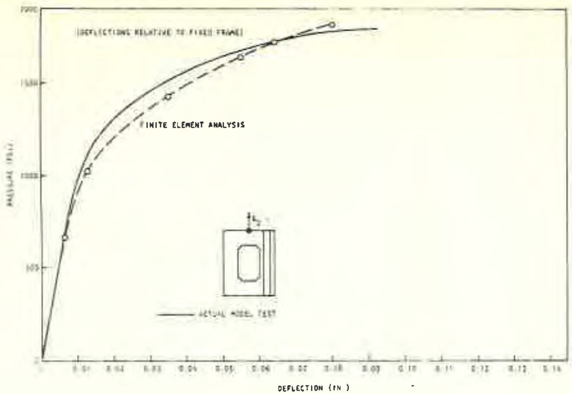

Fig 7(a) Pressure-Deflection Curve for Top Head of Hartlepool PCRV Model

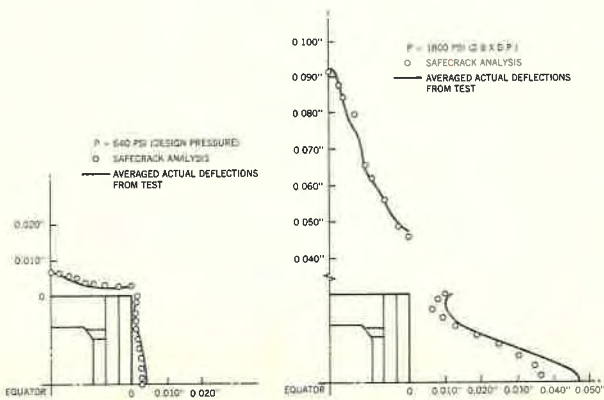

Fig 8 Typical Deflection Profiles of Hartlepool PCRV Model

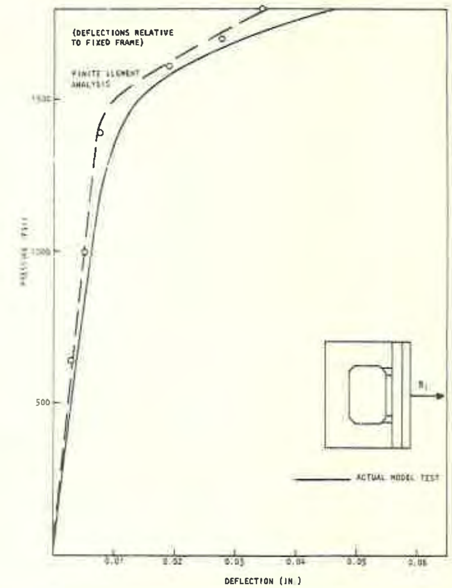

Fig 7(b) Pressure-Deflection Curve for Mid-Height of Wall of Hartlepool PCRV Model

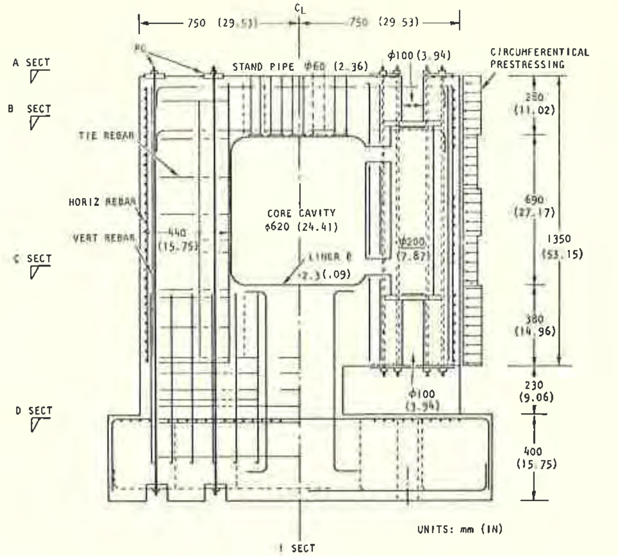

Fig 9(a) Ohbayashi-Gumi 1/20th Scale PCRV Model

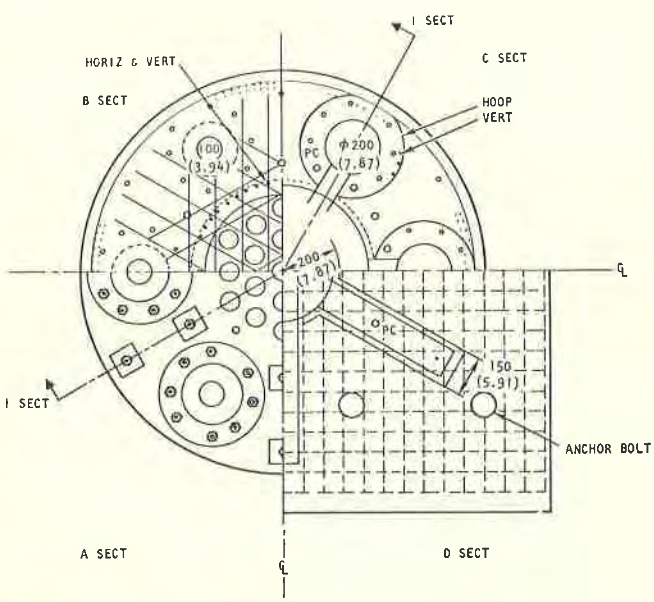

Fig 9(b) Ohbayashi-Gumi 1/20th Scale PCRV Model

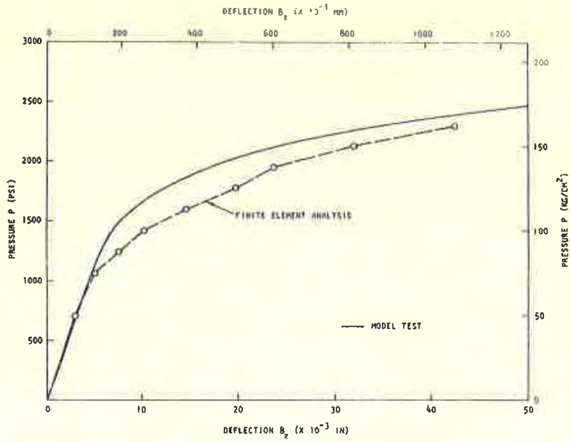

Fig 10(a) Pressure-Deflection Curve for Top Head of Ohbayashi-Gumi PCRV Model

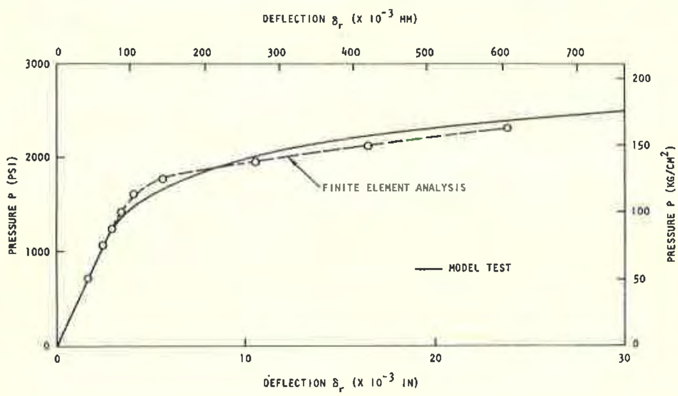

Fig 10(b) Pressure-Deflection Curve for Mid-Height of Wall of Ohbayashi-Gumi PCRV Model

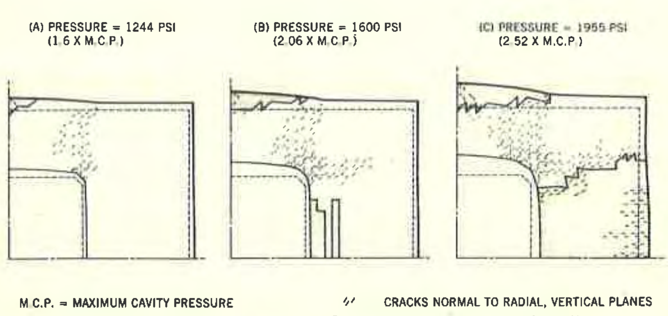

Fig 11 Typical Deflection Profiles and Cracking Patterns of Ohbayashi-Gumi PCRV Model